ELSEVIER

Journal of Applied Geophysics 50 (2002) 163–177

JOURNAL OF APPLIED GEOPHYSICS

www.elsevier.com/locate/jappgeo

Smooth and block inversion of surface NMR amplitudes and decay times using simulated annealing

O. Mohnke *, U. Yaramanci

Department of Applied Geophysics, Technical University of Berlin, Institut fur Angewandte Geophysik, Ackerstrasse 71-76, D-13355 Berlin, Germany

Abstract

This paper introduces a new 1-D inversion scheme for surface nuclear magnetic resonance (SNMR) amplitudes and decay times, using the optimized random search algorithm simulated annealing (SA). As an alternative to the smooth inversion used in other SNMR inversion techniques, the new scheme can also use block inversion, similar to 1-D geoelectrics. In smooth inversion, the number and thickness of inversion layers as well as the degree and type of the smoothness constraint, for example, the parameter of regularization, is most decisive on the results of the inversion. Therefore, the results are highly ambiguous, depending on the type and degree of regularization. To improve the mapping of aquifers with sharp boundaries and to overcome the ambiguity of the smooth inversion, a different approach has therefore been chosen, using block inversion. Using both smooth and block inversions, respectively, the results for two synthetic sets of SNMR data and for field data from a site in northern Germany with well-known hydrogeological properties are discussed. The results of block inversion and smooth inversion using a regularization that favors more block-like structures correspond to the sharp aquifer boundaries of the synthetic models and the site. The conventional smooth inversion gives only a rough estimate of the aquifer location.

Keywords: Surface nuclear magnetic resonance; Simulated annealing; Inversion

1. Introduction

Surface nuclear magnetic resonance (SNMR) is a non-invasive groundwater-exploration method allowing a direct determination of the water content and the permeability from the relaxation signal of excited hydrogen protons (Schirov et al., 1991; Legchenko and Shushakov, 1998; Yaramanci et al., 1999). The amplitudes and decay times of the relaxation signals are directly linked to the content of mobile water and to the pore sizes in the subsurface, respectively. In SNMR, the hydrogen protons of the pore fluid are excited with a primary magnetic field generated by a circular or figure-eight antenna loop. The exciting pulse oscillates with the local Larmor frequency of the protons. After termination of the excitation pulse, the responding magnetic field due to relaxation of the precessing hydrogen protons in the free pore water is then measured, using the same loop as receiver.

At present, the maximum depth of investigation of SNMR — limited due to the diameter of the antenna loop and the maximum applied intensity of excitation, that is, pulse moment — is approximately 100 m. So far, SNMR is used in sounding mode. Thus, the inversion of SNMR data is one-dimensional only.

* Corresponding author.
E-mail address: oliver.mohnke@tu-berlin.de (O. Mohnke).

0926-9851/02/$ - see front matter
PII: S0926-9851(02)00137-4

Available inversion schemes, for example, the NUMIS© program (Legchenko and Shushakov, 1998) or the Smooth Inversion Software Package SISP (Mohnke and Yaramanci, 1999a) that is discussed in the present paper use a regularized smooth inversion (Constable et al., 1987). Whereas NUMIS© uses a least-squares inversion, SISP makes use of simulated annealing (SA), a random search algorithm for global optimization problems. The inversion is carried out on the basis of a number of preset inversion layers that are fixed in position and size. To control the smoothness of the inversion, SISP allows a choice between two different types of regularization, favoring gradual or block-like changes in the distribution of water content and decay times, respectively.

An alternative approach to the smooth inversion of SNMR data is the use of block inversion (Mohnke and Yaramanci, 1999b) implemented in the Block Inversion Software Package (BISP). Similar to the inversion of 1-D geoelectrics or electromagnetics, BISP not only suits the water content and the decay time constant of each inversion layer, but also includes the layer thicknesses and boundaries for a given number of layers in the inversion process. In block inversion, regularization has negligible effects on the results except for very high degrees of regularization or high numbers of layers used.

To examine the quality and reliability of both smooth and block inversions of SNMR data, inversions of synthetic and field data are carried out and discussed with respect to their resolution and the inversion method.

2. Method

Magnetic resonance is based on the fact that many atomic particles have a magnetic dipole moment caused by their spin. Within the scope of surface nuclear magnetic resonance (SNMR), only the magnetic moments of atomic nucleons are of interest. Since pairs of protons and neutrons trend to align their angular moment in antiparallel form, the resulting dipole moment for small nuclei is given by the moment of the last non-paired nucleon. A water molecule H_2O consists of a single oxygen atom and two hydrogen atoms. The oxygen atom O having eight protons as well as eight neutrons does not have a resulting magnetic moment, whereas the hydrogen atom H with only one single proton has a magnetic moment. Hence, a water molecule has a magnetic dipole moment as well. This allows the use of the SNMR method as a geophysical technique to derive the amount of water in the subsurface.

In general, the magnetic moment of the water molecules is oriented parallel or antiparallel to the local geomagnetic field $\mathbf{B}_0$. The angular frequency of the hydrogen protons is given by

$$\omega_L = 2\pi f_L = \gamma_p \| \mathbf{B_0} \|, \quad (1)$$

where f_L is the local Larmor frequency of the protons and $\gamma_p = 0.267518$ Hz/nT is the gyromagnetic ratio. On application of a much smaller secondary magnetic field ($B_\perp \ll \| \mathbf{B}_0 \|$) perpendicular to $\mathbf{B}_0$ that oscillates with the local Larmor frequency, the vector of the magnetic moment is tilted away, precessing with ω_L around the axis of $\mathbf{B}_0$ and emitting a magnetic field response of its own. When the secondary field is terminated, the magnetic moments return to their initial position and the response field decays with a time constant T_2^* (spin–spin relaxation time). For SNMR measurements, this secondary excitation field is generated by a circular, square or figure-eight loop antenna energized by an alternating current

$$I(t) = I_0 \cos(\omega_L t). \quad (2)$$

The excitation intensity of the pulse is characterized by the pulse moment $q = I_0\tau$, where τ is the duration of the exciting pulse. After termination of the pulse, the voltage induced in the loop due to the relaxation of the excited hydrogen protons is given by

$$E(t,q) = E_0(q) e^{-t/T_2^*(q)} \cos[\omega_L t + \varphi(q)]. \quad (3)$$

While the initial amplitude E_0 at $t = 0$ (termination of the excitation pulse) is directly proportional to the water content, the decay time constant T_2^* is associated with the mean pore size and consequently linked to the grain size of the material (Kenyon et al., 1989).

The values for T_2^* range from less than 60 ms for clay and sandy clay up to 600–1000 ms for pure water, whereas 60–300 ms are typical for sands and 300–600 ms for gravel (Schirov et al., 1991; Yaramanci et al., 1999).

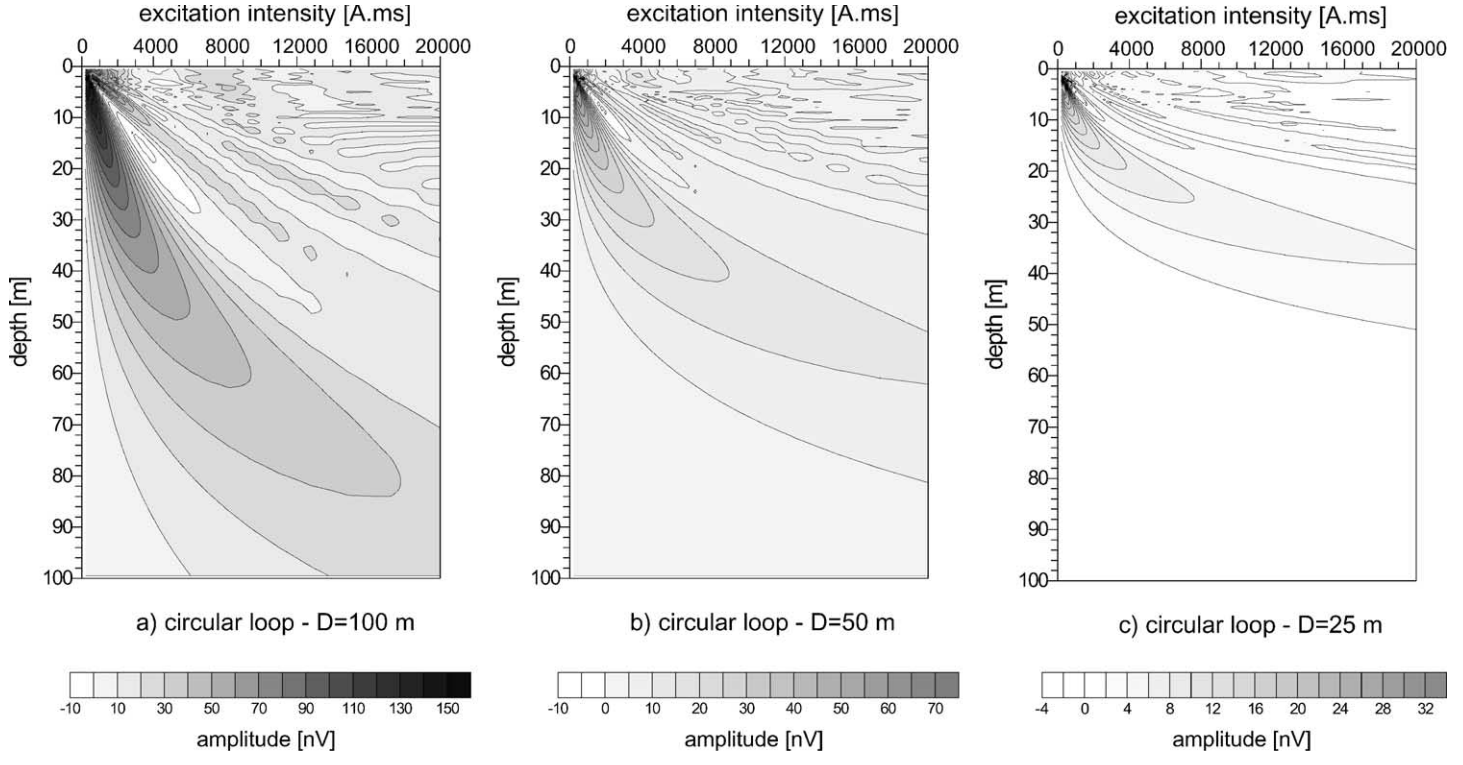

Fig. 1. Contribution to the SNMR signal amplitude of thin horizontal layers (0.5 m) at various depths and excitation intensities (pulse moments q) for a circular loop with a diameter of (a) 100 m, (b) 50 m and (c) 25 m. Earth magnetic field intensity: 48,000 nT, inclination: 60°.

According to Weichmann et al. (1999, 2000) and Mohnke and Yaramanci (1999b), the envelope of the relaxation signal can be expressed as

$$E_0(q)e^{-t/T_2^*(q)} = \omega_l M_0 \int_V B_\perp(\mathbf{r}) f(\mathbf{r}) e^{-t/T_2^*(\mathbf{r})} \sin[\theta(q)] d^3r. \quad (4)$$

M_0 is the macroscopic magnetic moment of the water molecules in equilibrium condition before the excitation pulse is applied. Note that Eq. (4) is only valid for the approximation of circular polarized magnetic fields. For highly conductive material, the effect of elliptic polarization of the corresponding fields has to be taken into account, as is shown by Weichmann et al. (2000). $B_\perp(\mathbf{r})$ is the component of the excitation field perpendicular to the local geomagnetic field for a unit current of 1 A. The tilt angle of the deflected hydrogen spins for a unit volume at the point $\boldsymbol{r}$ is given by

$$\theta(q,\mathbf{r}) = 0.5\gamma_p B_\perp(\mathbf{r}) q. \quad (5)$$

$f(\mathbf{r})$ is the water content, the parameter $T_2^*(\mathbf{r})$ characterizes the mean decay time constant of a unit volume at the point $\mathbf{r}$ in the subsurface.

The phase shift φ between the excitation signal given in Eq. (1) and the measured relaxation signal given in Eq. (3) is associated with the electrical conductivity of the medium. If the conductivity of the subsoil is negligible, for example, $\sigma \ll 0.01$ S/m, then the excitation field and the response field of the precessing hydrogen protons will have the same phase, thus $\varphi = 0$. For highly conductive media, both amplitude and phase of the signal are modified. Therefore, changes in φ indicate changes of the conductivity of the subsoil and groundwater, respectively. However, a quantitative interpretation of the phase of SNMR measurements has not been developed so far.

The intensity of excitation q $[A{\cdot}s]$ determines the depth of investigation, as it focuses the signal on a certain depth range; for higher pulse moments, the SNMR response originates from greater depths. With the existing equipment, pulse moments q range from 60 up to 20,000 A ms depending on the loop size and the electrical conductivity of the subsurface. In addition to the excitation intensity of the signal, the loop size is most decisive for the maximum depth of penetration. In Fig. 1, the distribution of the signal contribution from thin layers ($\Delta z = 0.5$ m) at depths from 0 to 100 m is plotted versus the intensity of excitation for three circular antennae with different loop diameters lying on a low conductive ground ($\sigma = 0.001$ S/m). The maximum depth of investigation decreases rapidly for smaller loop diameters. For a loop diameter $D = 100$ m, the maximum depth of investigation is approximately 70–80 m. For $D = 50$ m, it is about 50–60 m and for $D = 25$ m, it is 30–40 m. The depth of investigation can be decreased considerably in highly conductive media.

3. Forward modeling

At present, SNMR measurements are conducted in sounding mode. Therefore, the inversion of SNMR data is one-dimensional, that is, the water content and decay time distribution are only a function of depth z. This yields the following one-dimensional formulation of Eq. (4)

$$E_0(q)e^{-t/T_2^*(q)} = \int_0^\infty K(q,z) f(z) e^{-t/T_2^*(z)} \mathrm{d}z, \quad (6)$$

where the kernel function $K(q,z)$ is given by

$$K(q,z) = \omega_\mathrm{L} M_0 \int_{-\infty}^{\infty} \int_{-\infty}^{\infty} B_\perp(x,y,z) \sin[\theta(q)] \mathrm{d}x\, \mathrm{d}y. \quad (7)$$

For a numerical evaluation of the above equations, we discretize and parameterize z, $f(z)$ and $T_2^*(z)$ in Eqs. (6) and (7).

$$\begin{aligned} z \in [0,\infty) &\mapsto z \in \{z_0;\cdots,z_n;\cdots,z_N\} \\ f(z) &\mapsto f \in \{f_0;\cdots,f_n;\cdots,f_N\} \\ T_2^*(z) &\mapsto T_2^* \in \{T_{2_0}^*;\cdots,T_{2_n}^*;\cdots T_{2_N}^*\} \end{aligned} \quad (8)$$

In 1-D, the water content $f(z)$ and the decay time constant $T_2^*(z)$ have constant values within each layer in the interval $z \in [z_{n-1}, z_n)$ (basic layer). Thus, Eq. (6) can be written as

$$E_0(q)e^{-t/T_2^*(q)} = \sum_{n=1}^{N} \left\{ \int_{z_{n-1}}^{z_n} K(q,z) f_n e^{-t/T_{2_n}^*} \mathrm{d}z \right\}. \quad (9)$$

For sufficiently small basic layers, the kernel function $K(q,z)$ can be assumed to be constant in $z \in (z_{n-1}, z_n)$. Thus, Eq. (9) can be written as

$$E_0(q)e^{-t/T_2^*(q)} = \sum_{n=1}^{N} \{K(q,\tilde{z}) f_n e^{-t/T_{2n}^*}(z_n - z_{n-1})\} \quad (10)$$

where $\tilde{z}=(z_{n-1}+z_n)/(2)$ is the center depth of the nth basic layer.

Considering a complete SNMR sounding using K different pulse moments q_k for different sounding depths and N basic layers with constant values for f and T_2^*, Eq. (6) is written in matrix notation as

$$\underline{\underline{A}} \cdot \chi = \mathbf{e}. \quad (11)$$

The distribution of the water content and the relaxation parameters of a layered earth is then given by $(\chi = f_1 e^{-t/T_{21}^*}, \ldots, f_N e^{-t/T_{2N}^*})^{\mathrm{T}}$. The set of SNMR relaxation signals is written as $\mathbf{e}=(\boldsymbol{E}_0(q_1)e^{-t/T_2^*(q1)}, \ldots, E_0(q_k)e^{-t/T_2^*(qk)})^{\mathrm{T}}$. The superscript T denotes transposition. Each element $a_{kn}=K(q,\tilde{z})(z_n - z_{n-1})$ of the signal distribution matrix $\underline{\underline{A}}$ constitutes a hypothetical contribution to the SNMR signal of a corresponding basic layer n for a given pulse moment q_k. It is constant within an area having a constant earth magnetic field vector $\mathbf{B}_0$.

4. Inversion

At this point, the inversion of SNMR data poses basically a linear inverse problem for the determination of distribution of the water content and for resolving the decay time distribution. However, in consideration of a possible incorporation of other geophysical methods, for example, joint inversion with VES or TEM, which will pose a non-linear problem, the inversion is carried out on the basis of a global optimization approach, using an algorithm called simulated annealing (SA).

Simulated annealing is a technique that has attracted significant attention as being suitable for optimization problems of large scales, especially ones where a desired global optimum is hidden among many poorer local minima. At the heart of the method lies an analogy with thermodynamics, specifically with the way that liquids freeze and crystallize or metals cool and *anneal*. At high temperatures, the molecules of a liquid move freely with respect to one another. When the liquid is slowly cooled down, thermal mobility will be lost. The molecules are often able to line themselves up and form a pure crystal that is completely ordered over a distance up to billions of times the size of an individual molecule in all directions. This crystal represents the state of minimum energy for this system. The essence of this process is a sufficiently *slow* cooling, allowing ample time for the redistribution of the particles as they loose thermal mobility. The so-called Boltzmann probability distribution,

$$P \sim e^{-E/kT} \quad (12)$$

expresses the idea that a system in thermal equilibrium at the temperature T has its energy probabilistically distributed among all different energy states E. Even at low temperature, there is a chance—although very small—that the system is in a high state of energy. Therefore, there is a corresponding chance for the system to get out of a local energy minimum in favor of finding a better or global one. The parameter k is a constant of nature that describes the relation of temperature to energy. This means that the energy of the system can go upwards as well as it can go downwards. However, the lower the temperature, the less likely becomes an upward move. This kind of approach, called a *simulated annealing* process, was first incorporated in numerical calculations by Metropolis et al. (1953).

The inversion scheme introduced in the present paper uses a modified version of the Corona et al. (1987) implementation of SA. The SA algorithm explores the function's entire surface and tries to optimize the function while moving both uphill and downhill. Thus, it is largely independent of the starting model and can escape from local minima and go on to find the global minimum. Therefore, it is superior to conventional least-squares algorithms, but at the cost of increased computation time.

In consideration of the fact that a SNMR sounding consists of merely 10–20 single measurements to evade overdetermination, it is reasonable—though not necessary—to use a number of inversion layers less or equal than the number of layers used in the calculation grid according to Eq. (8). In case of an application of smooth inversion, these layers can be equidistant or increase in thickness with increasing depths—having, however, fixed layer boundaries and positions. For block inversion, the number of inversion layers will be constant, but the boundary of

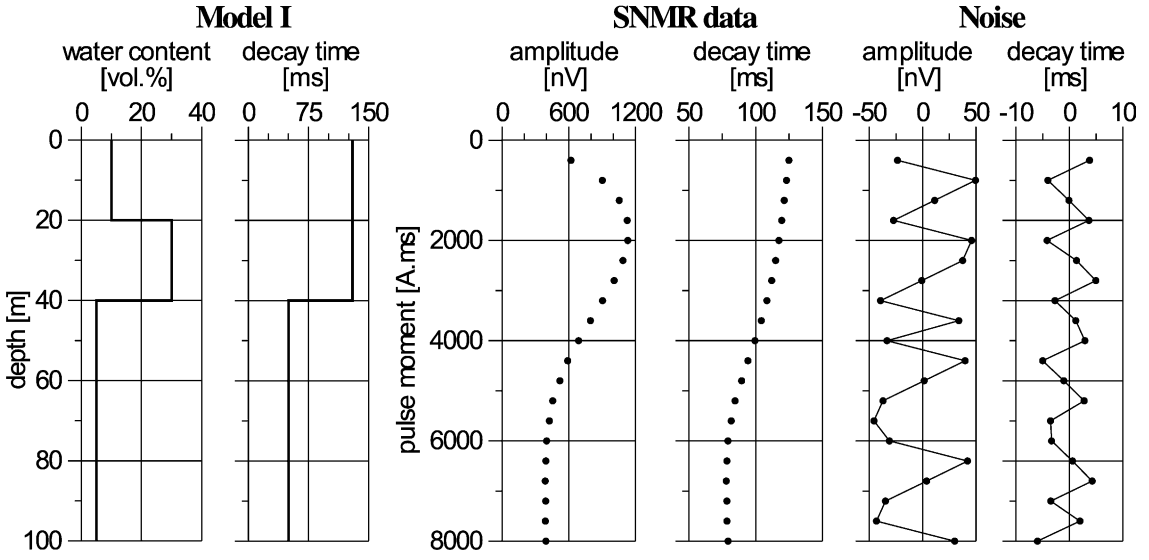

Fig. 2. Model I: Synthetic SNMR amplitudes and decay times (5% noise) for a single aquifer model with sharp boundary conditions.

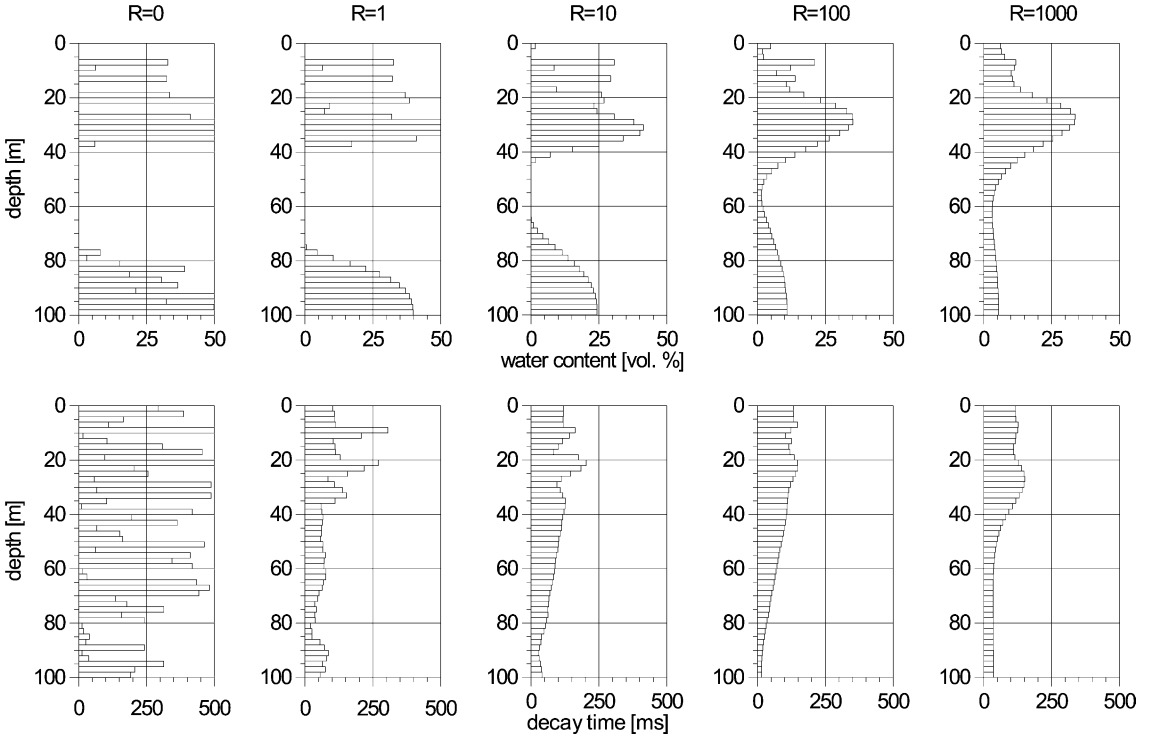

Fig. 3. Model I: Results of type I smooth inversion (SISP) for SNMR amplitudes and decay times for degrees of regularization from 0 to 1000.

each inversion layer is subject to the inversion as well as the water content and the decay time. The thickness of the mth inversion layer is given by

$$\Delta\hat{z}_m = \sum_{i=1}^{J} \Delta z_i, \tag{13}$$

in which J is the number of basic layers summarized in the mth inversion layer. The upper boundary of the respective inversion layer is then given by

$$\hat{z}_m = \sum_{i=2}^{m} \Delta\hat{z}_{i-1}. \tag{14}$$

To each of these so-defined M inversion layers, a water content $\hat{f}_m$ and a decay time $\hat{T}_m$ is assigned according to

$$\left.\begin{array}{l} f(z) = \hat{f}_m \\ T_2^*(z) = \hat{T}_m \end{array}\right\} \quad \text{with } (\hat{z}_m \le z < \hat{z}_{m+1}), \tag{15}$$

yielding vectorial expressions $\hat{\mathbf{f}} = (\hat{f}_1 \ldots, \hat{f}_M)^{\mathrm{T}}$ and $\hat{\mathbf{T}} = (\hat{T}_1, \ldots, \hat{T}_M)^{\mathrm{T}}$ for the distribution of the water content and decay time with respect to the user's choice of inversion layers.

The inverse problem is then solved basically by successively minimizing the two cost functions

$$\Gamma_1(\hat{\mathbf{f}}) = \| \mathbf{e}_{o_{\mathrm{obs}}} - \underline{\underline{A}} \cdot \chi \|_{L_2} + R \cdot \| \eta(\hat{\mathbf{f}}) \|_{L_p} \doteq \mathrm{Min}, \tag{16}$$

and

$$\Gamma_2(\hat{\mathbf{T}}) = \| \mathbf{T}^*_{2_{\mathrm{obs}}} - \mathbf{T}^*_{2_{\mathrm{calc}}} \|_{L_2} + R \cdot \| \eta(\hat{\mathbf{T}}) \|_{L_p} \doteq \mathrm{Min} \tag{17}$$

with $T^{*\,(i)}_{2_{\mathrm{calc}}} = -((t_1)/(\ln E^{(i)}_{t_{1\mathrm{calc}}} - \ln E^{(i)}_{0_{\mathrm{calc}}}))\eta$ is the vector minimizing the changes in the distribution of the water content, that is, regularization, and is generally given by

$$\eta(\mathbf{a}) = (a_1 - a_2, a_2 - a_3, \ldots, a_{i-1} - a_i, \ldots, a_{M-1} - a_M)^T, \tag{18}$$

where $\mathbf{a}$ is of the dimension M and η is of the dimension $M-1$. The parameter R controls the degree of the smoothness constraint η.

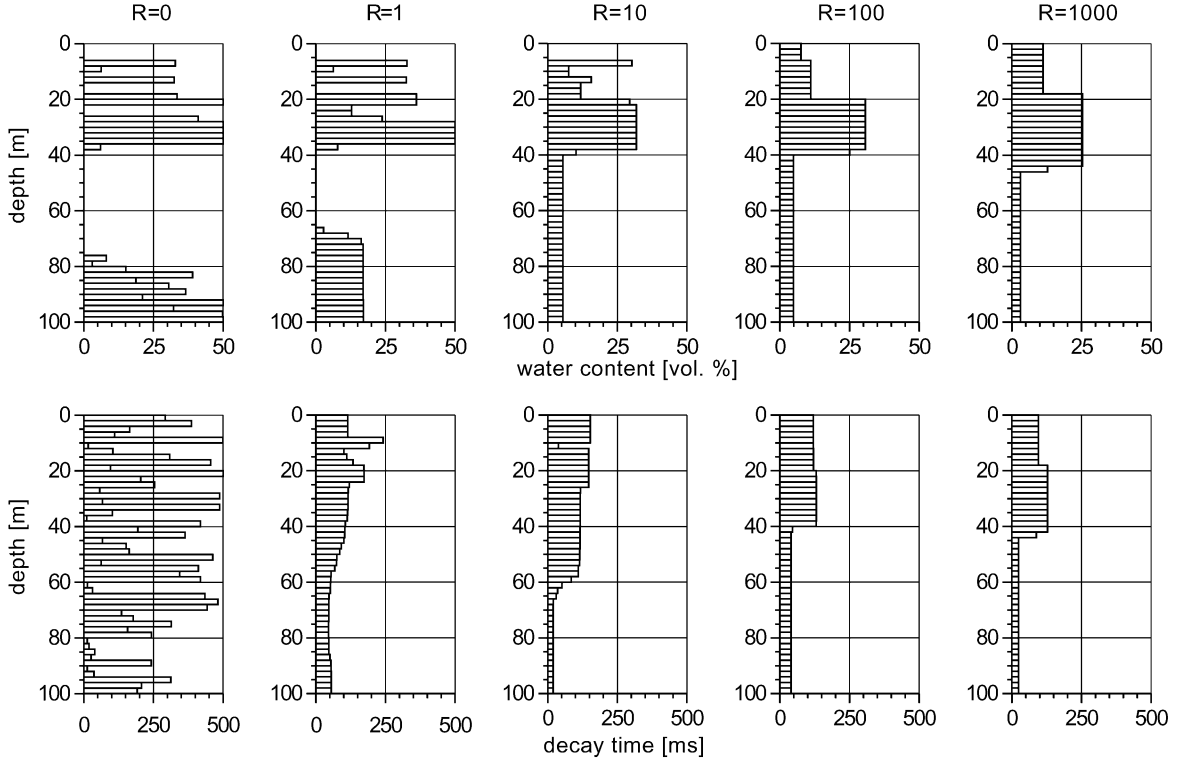

Fig. 4. Model I: Results of type II smooth inversion (SISP) for SNMR amplitudes and decay times for degrees of regularization from 0 to 1000.

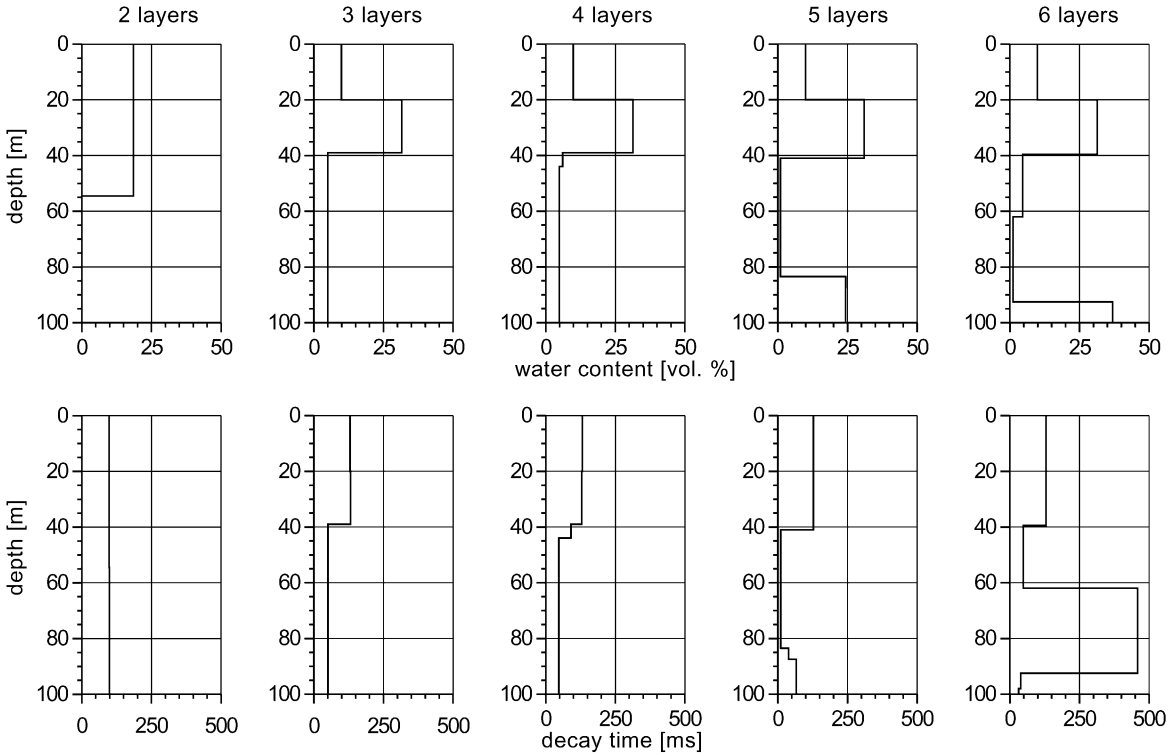

Fig. 5. Model I: Results of block inversion (BISP) for SNMR amplitudes and decay times for various numbers of inversion layers.

A new feature in this respect is that it is possible to use different types of regularization, depending on the normalization L_ρ. Using L_2 normalization ($\rho = 2$) in Eqs. (16) and (17), the differences between the water contents and decay time constants of neighboring layers are conditioned with their second power (inver-

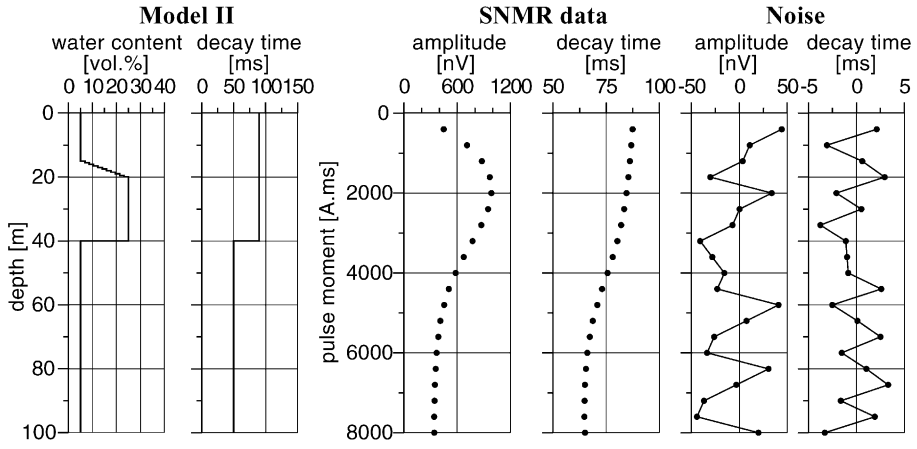

Fig. 6. Model II: Synthetic SNMR amplitudes and decay times (5% noise) for a single aquifer model with a large capillary zone and a sharp lower boundary.

sion of type I). This is a standard regularization, as is used in other applications for the inversion of SNMR data as well (Schirov et al., 1991); it favors smoothness in the sense of gradual changes of the water content and decay time constants.

A different effect of the term of regularization can be attained using L_1 normalization ($\rho = 1$) of the constraining vector η (inversion of type II). Here, the differences in the layer properties are conditioned using their absolute value favoring just a few changes with high contrasts and a constant level in-between, hence causing a more block-like distribution of the water content and decay time constants, respectively.

The strategy for the smooth inversion process used in SISP is separated into two consecutive steps, both of which use the same fixed division of inversion layers and a particular type of regularization. The first step of the inversion is the determination of the water content according to Eq. (16). Based on the results of this step, in the second step, the inversion of the decay time constants is conducted, using a second amplitude value of the relaxation signal at the time t_1, for example, $t_1 = 30$ ms, in accordance with Eq. (17).

In block inversion (BISP)—similar to the smooth inversion process—the determination of the water content and decay time distribution is done in two consecutive steps, which are (a) inversion of the initial amplitude for the determination of the water content, and (b) the inversion of the decay time constants for the determination of the decay time distribution in the subsurface. However, since for block inversion the layer boundaries $\hat{z}$ are subject to the inversion process, too, the distribution of inversion layers stated in Eqs. (13)–(15) has to be readjusted for each iteration of the inversion process. Since the SA algorithm used only employs forward calculations, these adjustments are easily incorporated.

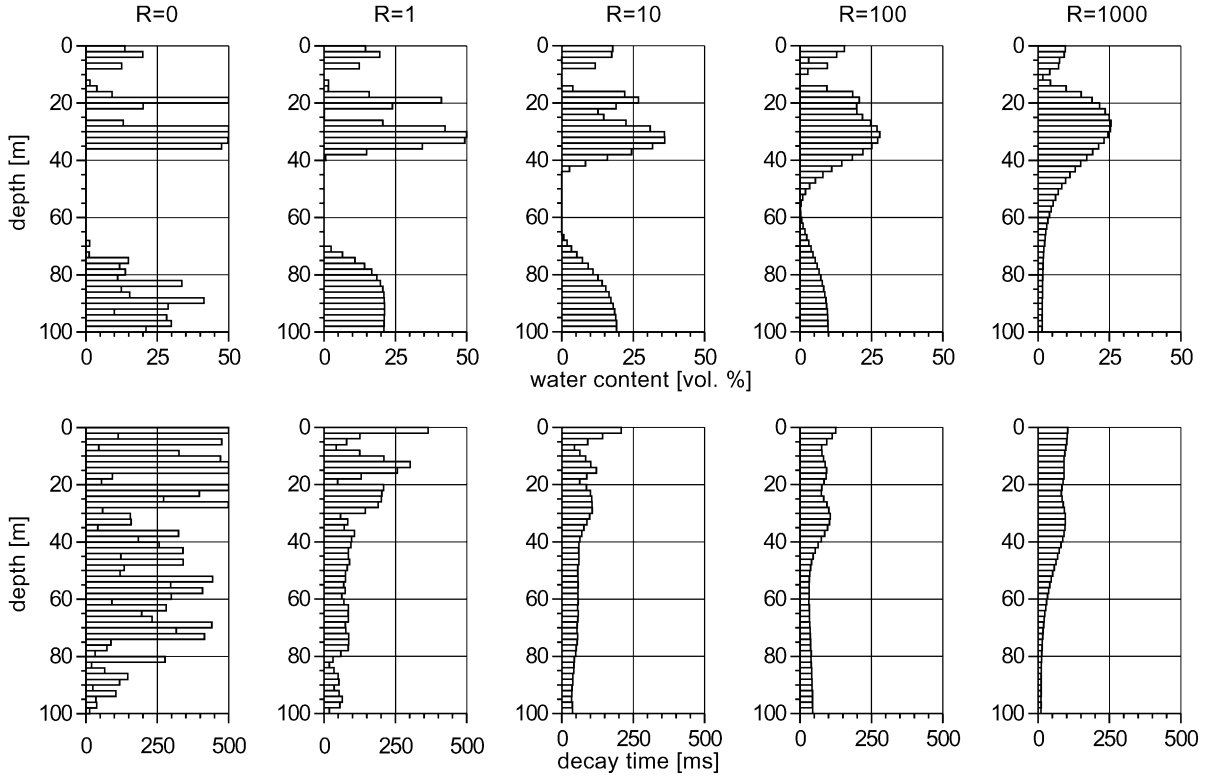

Fig. 7. Model II: Results of type I smooth inversion (SISP) for SNMR amplitudes and decay times for degrees of regularization from 0 to 1000.

5. Tests with synthetic data

Both smooth and block inversion schemes have been tested with synthetic data. Inversions for two different hydrogeological scenarios are presented, calculated for a circular loop antenna with a diameter of 100 m in a geomagnetic field of 48,000 nT at an inclination of 60°. The vertical calculation grid is set to 0.5 m with a maximum depth of 100 m. The first model in Fig. 2 describes the scenario of a single aquifer with a sharp upper boundary at 20 m as well as a sharp lower boundary at 40 m and 30 vol.% of mobile water. This scenario would be consistent with a geology of medium sand layers having decay times of about 130 ms lying on a clay aquiclude with corresponding decay times of 50 ms (Schirov et al., 1991; Yaramanci et al., 1999). The synthetic amplitudes and decay times shown in Fig. 2 are superimposed with 5% random noise. Plotted in Figs. 3 and 4 are the inversion results of the smooth inversion of type I (Fig. 3) and type II (Fig. 4) using various degrees of regularization ($R = 0$, 1, 10, 100, 1000). The inversion grid employed consists of 50 equidistant layers with a thickness $\Delta z = 2.0$ m.

For a small degree of regularization ($R < 100$), both the smooth inversion type I and type II fail to resolve the three-layer structure of the model. Besides a slight indication of the aquifer from the model, a second aquifer forms between 70 and 100 m. This is an artifact due to the applied noise and the low sensitivity of the loop configuration used for these depths.

Using a higher degree of regularization ($R \geq 100$), the smooth inversion type I yields a good estimation of the aquifer location between 20 and 40 m depth with a water content of about 33 vol.% and decay times of 100 ms. However, the algorithm is not successful in determining the angular geometry of the aquifer. The results of the smooth inversion of

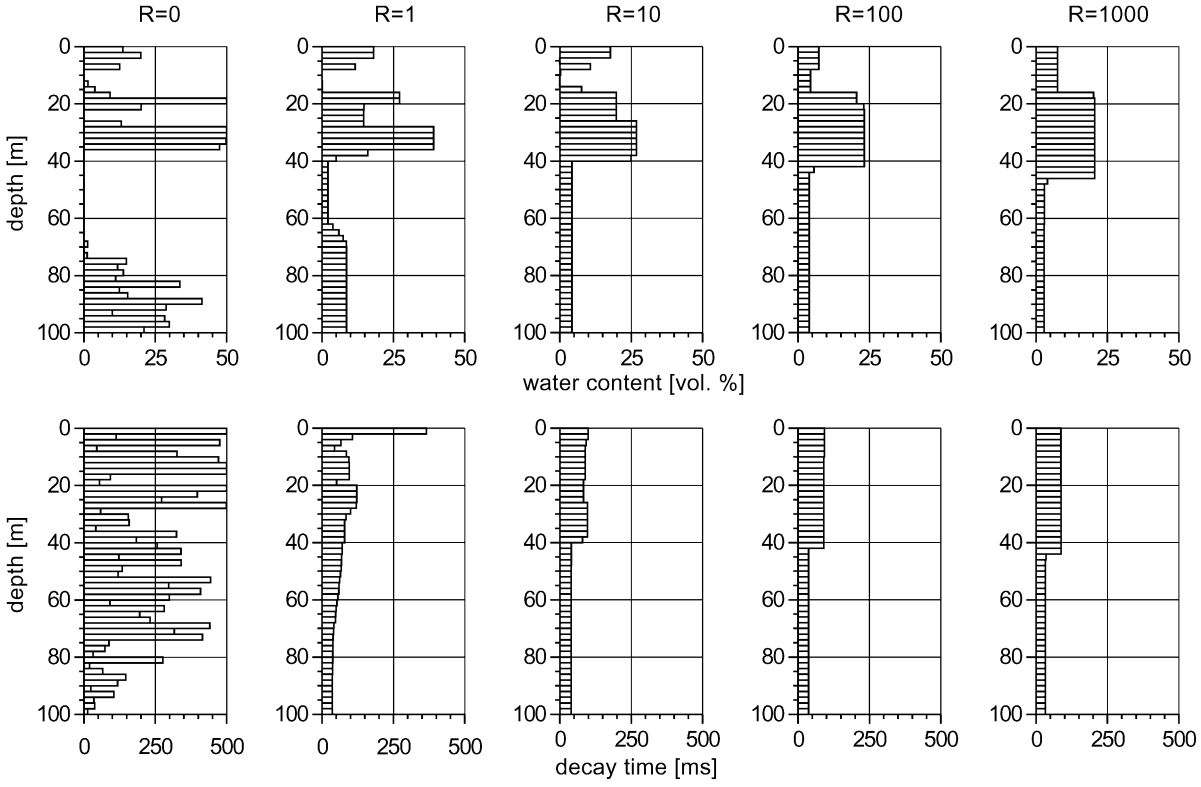

Fig. 8. Model II: Results of type II smooth inversion (SISP) for SNMR amplitudes and decay times for degrees of regularization from 0 to 1000.

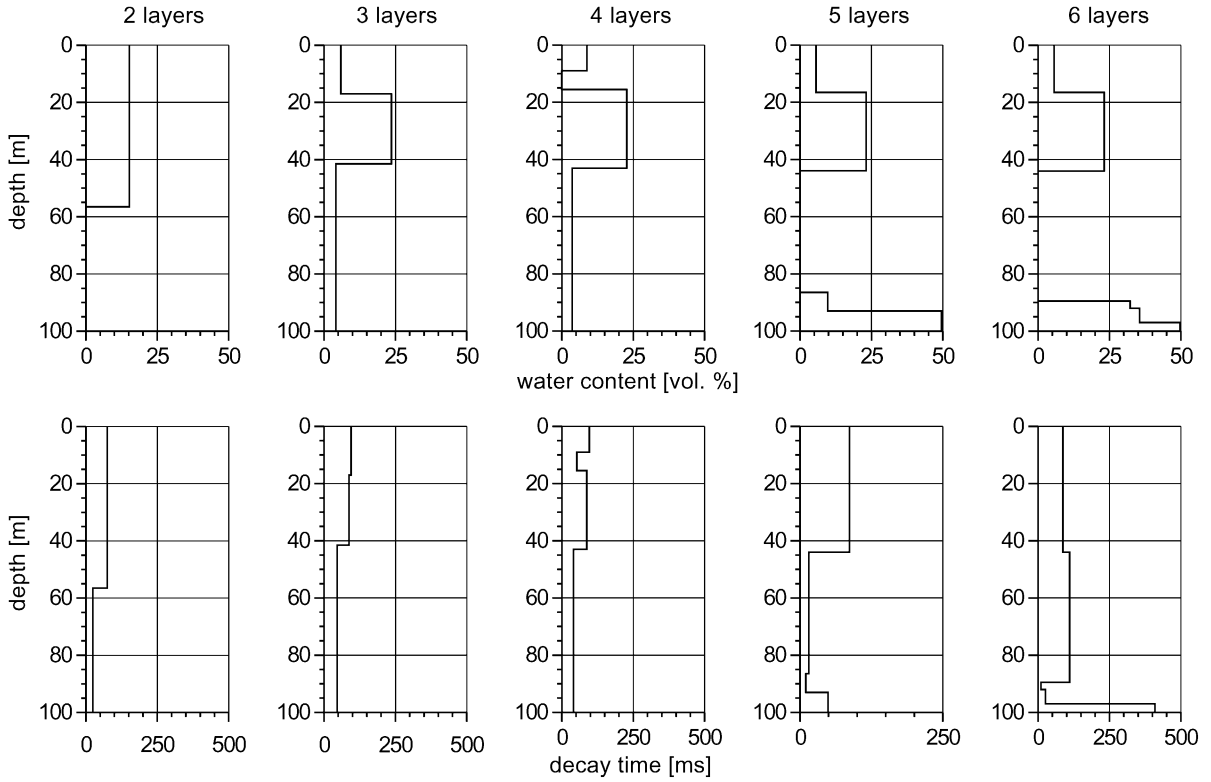

Fig. 9. Model II: Results of block inversion (BISP) for SNMR amplitudes and decay times for various numbers of inversion layers.

type II are more realistic in this respect and can determine the location and geometry of the aquifer as well as the water content and decay time distribution — however, only for a particular degree of regularization ($R = 100$). For all inversions presented, the root mean square error (rms) of the data fit is generally the same at about 5%, being the level of the random noise.

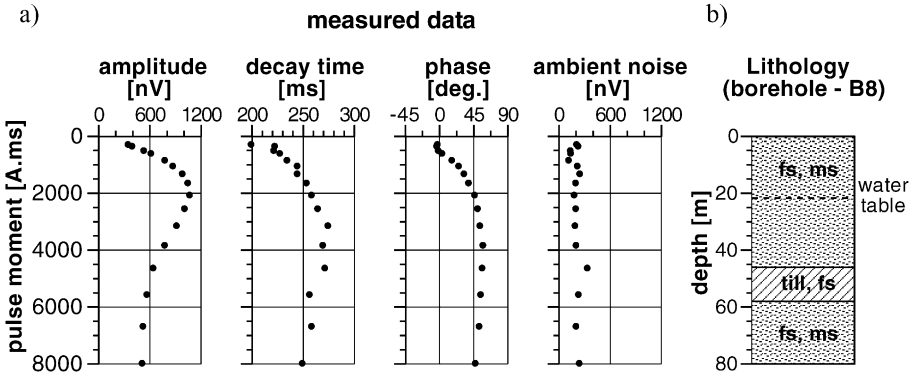

Fig. 10. (a) Measured SNMR data in Haldensleben (Germany) at location B8. (b) Lithology and water table for location B8 in Haldensleben (fs: fine-grained sand; ms medium-grained sand).

The results for the block inversion using up to six inversion layers are shown in Fig. 5. The results using three to six inversion layers correspond well to the sharp boundaries of the aquifer and prove to be stable regardless of the number of layers used. There is no need to apply an additional regularization term. However, when using larger numbers of inversion layers, the results become subject to regularization as well (Mohnke and Yaramanci, 1999b). The results using five and six inversion layers respectively show an artificial second aquifer beyond 70 m depth, due to the same effects as mentioned above. The second model presented in Fig. 6 also describes a single aquifer system, but unlike in the first model, we included a large capillary zone ranging from 15 to 20 m depth, due to smaller pore sizes and a sharp lower boundary at 40 m, with 25% of mobile water in the saturated zone. This would be consistent with a fine sand layering corresponding to a decay time $T_2^* = 90$ ms on top of clay layers with decay times of 50 ms. As for model I, 5% random noise has been added to the synthetic SNMR data.

The results of the smooth inversions using type I regularization have been plotted in Fig. 7 and for type II in Fig. 8. The results of the smooth inversion of type I using a degree of regularization $R \geq 100$ yield a good estimate of the aquifer location and properties, and get a good fit corresponding to the capillary zone of the model. However, the algorithm fails to find the correct location of the sharp lower boundary to the aquiclude at a depth of 40 m. Both the smooth inversion of type II and the block inversion shown in Fig. 9 can determine the sharp lower boundary of the aquifer. However, they always fail to determine the gradual changes of the water content in favor of a sharp upper aquifer boundary in the middle of the capillary zone at a depth of 17.5 m.

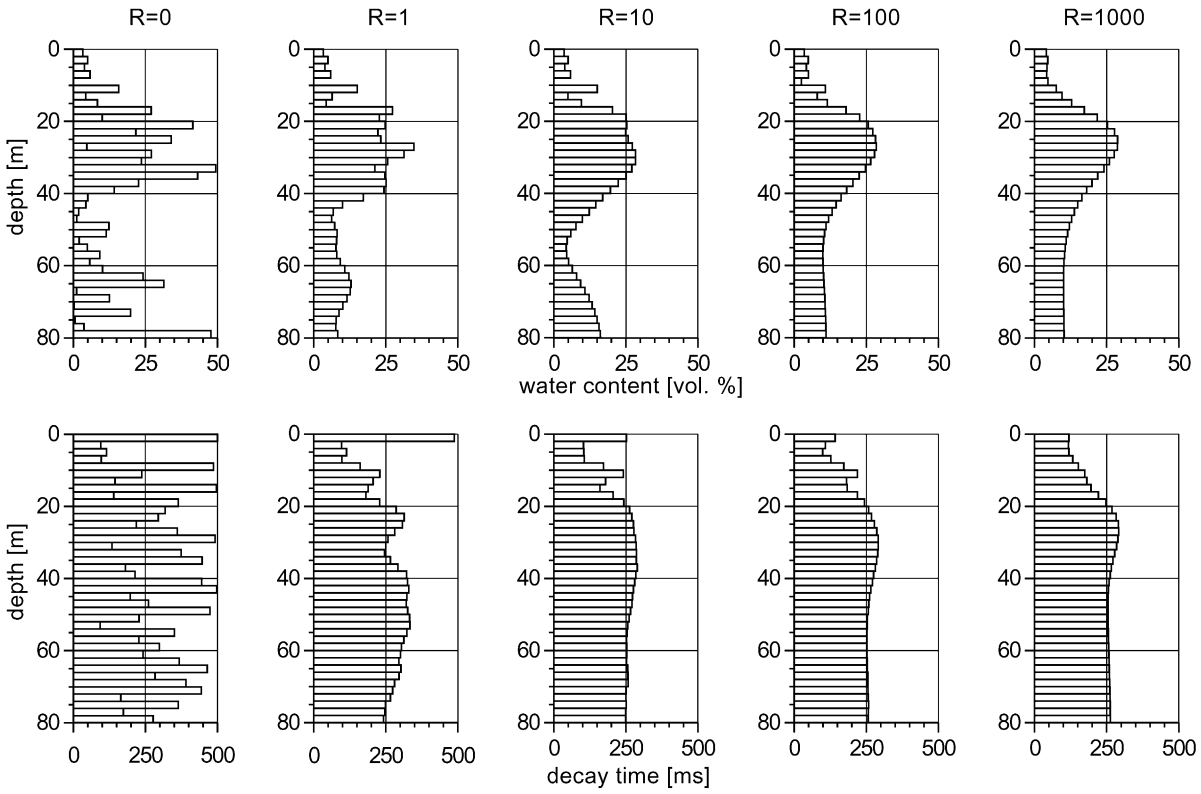

Fig. 11. Results of type I smooth inversion (SISP) for SNMR amplitudes and decay times at the location B8 in Haldensleben for degrees of regularization from 0 to 1000.

6. Field case—Haldensleben

Inversions have been carried out for data obtained from a SNMR sounding (Fig. 10a) at a site near Haldensleben in northern Germany (Yaramanci et al., 1999). The measurements were conducted using a circular antenna loop with a diameter of 100 m and a maximum pulse moment of $q = 7977$ A ms. The local geomagnetic field intensity was 48771 nT with an inclination of 64°. The signal amplitudes are typical of a sounding curve of a single aquifer at a moderate depth with a maximum amplitude of 1100 nV at a pulse moment $q = 2000$ A ms. The level of ambient noise is about 100–300 nV. The decay times, starting at 210 ms, gradually increase up to 280 ms at $q = 3000$ ms and slightly decrease to 250 ms at $q = 7977$ A ms. The phase slowly increases from 0° up to 60° at $q = 7977$ A ms, indicating the existence of conductive layers in the subsurface.

The geology of the area consists of an interbedding of well-sorted sands and Quaternary layers (Fig. 10b). At this site, borehole measurements confirmed a three-layer case with a single aquifer between 21.7 and 46 m having a sharp upper boundary due to a very small capillary zone as well as a sharp lower boundary to glacial till and about 30% mobile water. The conductivity of the subsurface is generally less than 0.005 S/m.

The inversion grid used consists of 40 equidistant layers ($\Delta z = 2.0$ m) with a maximum depth of 80 m. Shown in Fig. 11 are the results of the smooth inversion of type I for different degrees of regularization ($R = 0, 1, 10, 100, 1000$). For a degree of regularization between 100 and 1000, the inversion yields a rough estimation of the aquifer location between 18 and 40 and determines a water content of 28 vol.%. The smooth inversion of type I fails to render the sharp boundaries of the aquifer. The results of type II smooth inversion

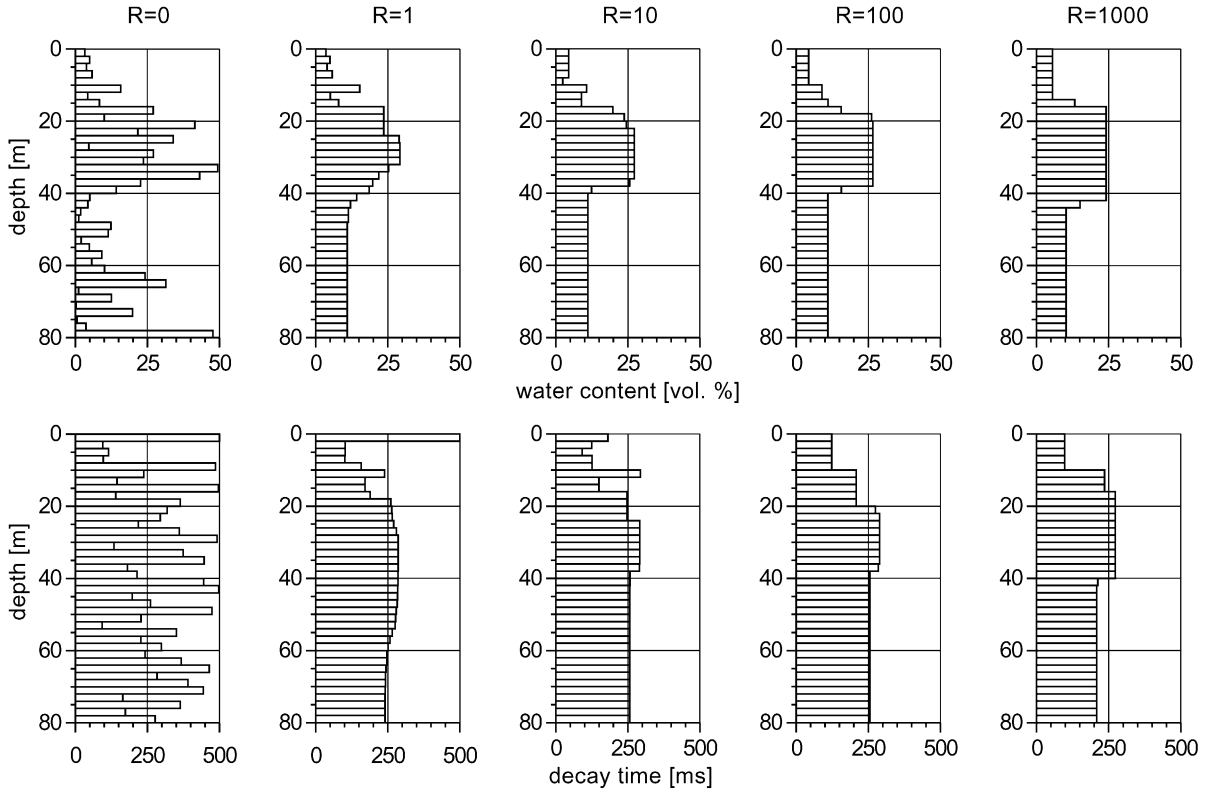

Fig. 12. Results of type II smooth inversion (SISP) for SNMR amplitudes and decay times at location B8 in Haldensleben for degrees of regularization from 0 to 1000.

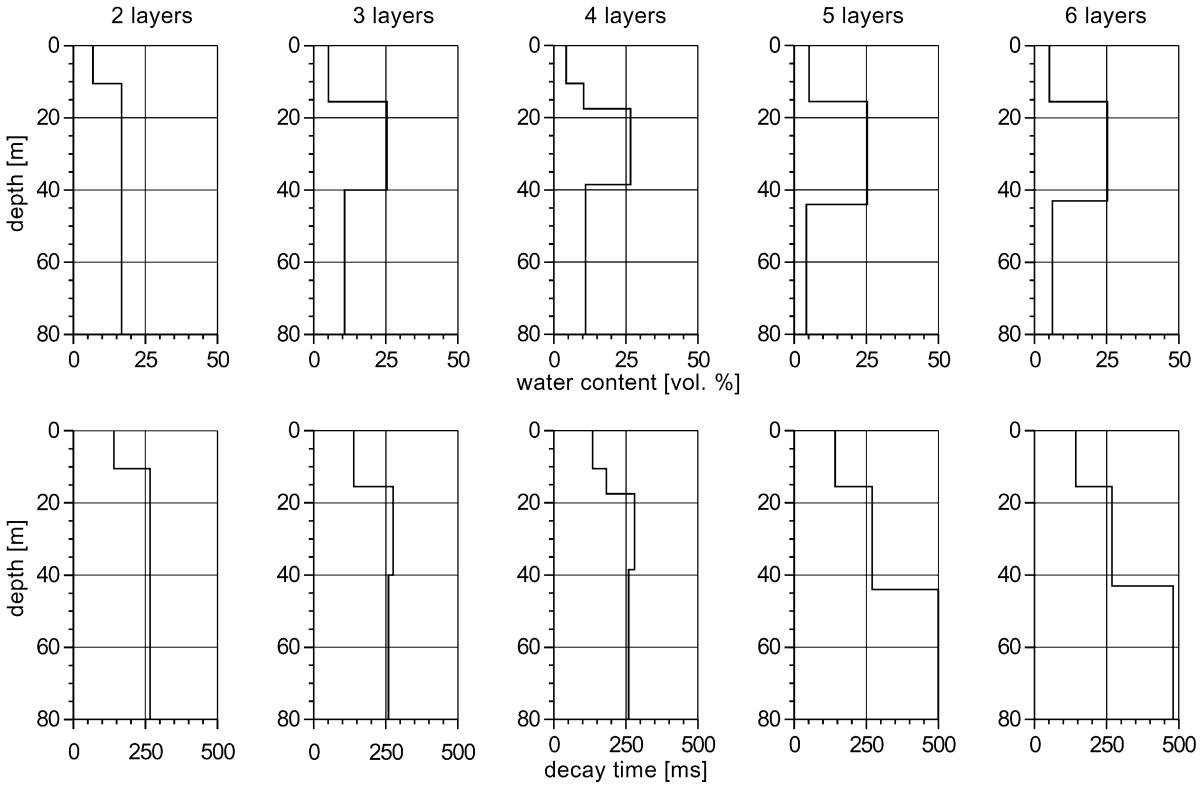

Fig. 13. Results of block inversion (BISP) for SNMR amplitudes and decay times at location B8 in Haldensleben for various numbers of inversion layers.

plotted in Fig. 12 are more realistic in this respect—only for a high degree of regularization, however. The results of the block inversion shown in Fig. 13 correspond to the known sharp boundaries of the aquifer and the results prove to be stable considering the number of layers used in the inversion. For all inversions carried out, the rms error of the data fit for amplitudes and decay times is generally less than 4%. However, both the smooth and the block inversion slightly underestimate the water content of the aquifer and only indicate the expected decrease of the decay time distribution due to the glacial till at a depth of below 46 m. The aquifer could be identified within reasonable limits for all inversion schemes examined in this study. However, the results are only in moderate agreement with the borehole measurements regarding the underestimation of the water content and the decrease of the decay time as a consequence of the glacial till between 46 and 59 m. The cause for this discrepancy is not yet fully understood, and further investigations on this matter are definitely required.

7. Conclusions

The presented inversion scheme for surface NMR with simulated annealing has considerable advantages, as it allows free choice of inversion parameters. Two different approaches to the inversion of SNMR data are available, using block inversion and two different types of smooth inversion. Furthermore, the simulated annealing algorithm used allows an easy incorporation of additional geophysical methods for a joint inversion, for example, VES or TEM. Considering the smooth inversion scheme, the parameter of regularization is highly decisive on the inversion results. Therefore, the recommendation is to carry out a variety of inversions with different degrees *R*

of regularization to test the geological plausibility of the results. The rms error is not implicitly a reliable criterion in this context!

If thin, equally thick inversion layers are used instead of layers that increase in thickness with depth as used in other applications for inversion of SNMR data, the results are less limited by the choice of model parameters, for example, layer boundaries. In this context, the effect of overdetermination is avoided using an adequate degree of regularization. For aquifers with sharp boundaries, it is preferable to employ smooth inversion using a regularization of type II that favors sharp contrasts in the distribution of the water content and decay times, respectively.

Block inversion, on the other hand, has some significant advantages. It inverts boundary depths and permits as well easy incorporation of a priori information, for example, incorporation of known layer boundaries obtained from other methods. There is no limitation due to the use of preset inversion layers; therefore, it allows a more natural interpretation especially for aquifers with sharp boundaries. Furthermore, there is no need for regularization in block inversion and thus this approach can reduce the ambiguity of the interpretation of SNMR data.

Acknowledgements

The authors thank P. Weidelt for providing the routines for the calculation of magnetic fields in layered conductive media and the anonymous reviewers for their work.

References

Constable, S.C., Parker, R.L., Constable, C.G., 1987. Occam's inversion: a practical algorithm for generating smooth models from electromagnetic sounding data. Geophysics 52, 289–300.

Corona, A., Marchesi, M., Matrini, C., Ridella, S., 1987. Minimization multimodal functions of continuous variables with the simulated annealing algorithm. ACM Transactions on Mathematical Software 13 (3), 262–280.

Kenyon, W., Howard, J., Sezginer, A., Straley, C., Matteson, A., Horkowithz, K., Ehrlich, R., 1989. Pore-size distribution and NMR in microporous cherty sandstones, 30th Annual Logging Symposium, Paper LL Trans. SPWL.

Legchenko, A., Shushakov, O., 1998. Inversion of surface NMR data. Geophysics 63, 75–84.

Metropolis, N., Rosenbluth, A., Rosenbluth, M., Teller, M., Teller, E., 1953. Equation of state calculations by fast computing machines. Journal of Chemical Physics 21, 1087–1090.

Mohnke, O., Yaramanci, U., 1999a. A new inversion scheme for surface NMR amplitudes using simulated annealing. Proceedings of the 61st EAGE Conference. EAGE, pp. 262–280.

Mohnke, O., Yaramanci, U., 1999b. Block inversion of surface NMR data using simulated annealing. Proceedings of 60st EEGS Conference. EAGE, pp. 262–280.

Schirov, M., Legchenko, A., Creer, G., 1991. A new direct noninvasive groundwater detection technology for Australia. Exploration Geophysics 22, 333–338.

Weichmann, P.B., Lavely, E.M., Ritzwoller, M., 1999. Surface nuclear magnetic resonance imaging of large system. Physical Review Letters 82 (20), 4102–4105.

Weichmann, P.B., Lavely, E.M., Ritzwoller, M., 2000. Theory of surface nuclear magnetic resonance with applications to geophysical imaging problems. Physical Review E 62 (1), 1290–1312, Part B.

Yaramanci, U., Lange, G., Knoedel, K., 1999. Surface NMR within a geophysical study of the aquifer at Haldensleben (Germany). Geophysical Prospecting 47, 923–943.